Corrosion Behaviour of Coatings on 304 Steel

AYSEL BÜYÜKSAGIS[1,*], UGUR ÖZTÜRK[1] and A. ABBAS AKSÜT[2]

[1]Science and Art Faculty, Afyonkarahisar Kocatepe University, Afyonkarahisar, Turkey
[2]Science Faculty, Ankara University, Ankara, Turkey

*Corresponding author: E-mail: absagis@aku.edu.tr

The aim of this study is to determine the corrosion characteristics of 304 steel by the methods of Tafel extrapolation, linear polarization and electrochemical impedance spectroscopy (EIS). The steel surface is covered with nickel as electrochemical Watt's bath. Additionally, polyaniline (PANI) is synthesized on the steel electrode covered with nickel by the method of electrochemical cyclic voltammetry method. The effect of single and double coats of steel on corrosion resistance is examined in 3.5 % NaCl, 1N NaOH and 1N HCl solutions for the waiting time of 1, 48, 120 and 168 h. The surface morphology of steel, which is uncovered, is examined by SEM-EDX and the polyaniline is also examined in the same way. As well as the one covered with Ni + polyaniline is examined in the same way too. The synthesized polyaniline on the surface is analyzed by FTIR spectrum. Double coatings (Ni + polyaniline) has showed better corrosion resistance than single coating (polyaniline). Ni + polyaniline coatings in 1 N NaOH and 1 N HCl solutions has showed better corrosion resistance than polyaniline coating. The corrosion current of the steel covered with Ni + polyaniline in 1 N HCl and 1 N NaOH solutions is lower than the corrosion current of polyaniline coating. SEM-EDX analyses have showed that the surface covered with Ni + polyaniline is more homogenous and compact. This result is also convenient with the electrochemical experiment results.

Key Words: Polyaniline, Corrosion, Cyclic voltammograms, Ni plate, Conductive polymer, Steel.

INTRODUCTION

There is growing interest relating research and industry to protect stainless steel against corrosion by means of polyaniline (PANI). This interest stems from the potential use of this coating in electronic applications such as batteries[1-3], electrochromic devices[4] and electronic displays[5]. Polyaniline is produced from an aqueous solution employing an acid-aniline mixture. In situ oxidation of aniline to form polyaniline is dependent upon several variables such as composition of the acid, nature of the oxidant, rate of oxidation, temperature and pH[6,7]. Sazou and Georgolios[8] claim these acids to result in poor adhesion of polyaniline layers on steel. Only dibasic acids such as oxalic acid are shown to provide adequate adhesion of polyaniline on steel. Camalet *et al.*[9] also showed that passivation of the steel prior to aniline polymerization is necessary to obtain adequate adhesion of the polyaniline coating. Martyak *et al.*[10] reported that, poor adhesion of polyaniline (polyaniline) is observed if the steel is not properly passivated. After polyaniline deposition, the Fe(III) layer is reduced to Fe(II) on the reverse scan but the adhesion of the polyaniline coating is excellent. Thompson *et al.*[11] proposed mechanisms for the corrosion protection of mild steel by both doped and de-doped forms of polyaniline in brine solutions and dilute hydrochloric acid. Ahmad and MacDiarmid[12] showed that emeraldine base deposited chemically on stainless steel prior to be treated with acids or metal chelating agents protects the metal surface from corrosion in chloride containing acid media. The formation of specific oxide layers occur when the polymer is formed on the surface during galvanostatic deposition. Many other publications have reinforced the importance of polyaniline for the corrosion protection of steels[13-16]. Camalet *et al.*[9] observed the passivation of steel by oxalate during the deposition of polyaniline in oxalate acid solution. Over the years, a number of important patents on the protection of steels by polyaniline have appeared[17-19].

The aim of this study is to determine the corrosion characteristics of 304 steel by the methods of Tafel extrapolation, linear polarization and electrochemical impedance spectroscopy (EIS). The polyaniline, which is a conductive polymer, is synthesized on the steel surface by the way of electrochemical cyclic voltammetry method. The steel surface is covered with nickel as electrochemical Watt's bath. Additionally, polyaniline is synthesized on the steel electrode covered with nickel by the method of electrochemical cyclic voltammetry method. The effect of single and double coats of steel on corrosion

resistance is examined in 3.5 % NaCl, 1N NaOH and 1N HCl solutions for the waiting time of 1, 48, 120 and 168 h. The surface morphology of steel, which is uncovered, is examined by SEM-EDX and the polyaniline one is also examined in the same way. And the one covered with Ni + polyaniline is examined in the same way too. The synthesized polyaniline on the surface is analyzed by FTIR spectrum. The film thickness occurred on the surface is measured by optic micrometer.

EXPERIMENTAL

Standard one-compartment three-electrode cells were used. The reference electrode was Hg/Hg_2Cl_2 (sat., KCl) and the counter electrode was a platinum sheet. In this study, all electrode potential values were referred to this reference electrode. The working electrodes were stainless steel samples (304) of 0.2826 cm^2 in electrode area embedded in polyester. The chemical compositions of (% w) the working electrode was given in Table-1.

TABLE-1
CHEMICAL COMPOSITIONS (% w) OF
WORKING ELECTRODE

Fe	70.55	Mn	1.50
Cr	18.45	Mo	0.48
C	0.08	Cu	0.48
Si	0.48	Ni	8.56
P	0.02	N	0.48
S	0.29	–	–

Gamry reference 600 potentiostat/galvanostat/ZRA system (Gamry Inc., USA) was used for potential-controlled polarization measurements. This system was interfaced to a personal computer to control the experiments which were controlled and the data were analyzed by using a Gamry framework/Echem analysis software. Aniline was freshly distilled and stored in the dark (Merck). All the other chemicals were analytical grade from Merck and used as received. The electrodes surfaces were polished mechanically using metallurgical papers of successive grades (120, 600 and 1200 μm) prior to each experiments (to remove any existing passive film). Then the electrodes were washed with 1/1 acetone-alcohol mixture and double distilled water (at 30 ºC for 15 min) by using Bandelin ultrasonic bath. After then cleaning the surface, specimens were dried at 40 ºC for 1 h.

Electropolymerization and electrochemical measurements: Polyaniline films were electrochemically deposited on stainless steel (SS) electrode applying at 50 mV s^{-1} in the 0.1 M aniline solution containing 0.3 M oxalic acid. The growths of polyaniline film were carried out in the potential range between -0.45 and 0.95 V applying 50 cycles for, the polyaniline coated electrodes were rinsed with double distilled water and then dried at 40 ºC for 1 h. Nyquist plots were recorded at various open circuit potentials after 0.5 h in 1N HCl, % 3.5 NaCl and 1N NaOH solutions. In order to characterize the protection mechanism of polyaniline on stainless steel, EIS measurements were obtained in the frequency range from 1×10^4 to 1×10^{-1} Hz by using an amplitude of 10 mV.

Nickel electrochemical deposition: Watts's bath was used as electrolyte and a standard DC power supply (SHENZEN MASTECH HY 3003-3 model) with variable potential was used as a power source. The chemical compositions of Watt's bath was given in Table-2.

TABLE-2
CHEMICAL COMPOSITIONS OF WATT'S BATH

Compounds	
$NiSO_4 \cdot 7H_2O$ (g/L)	300
$NiCl_2 \cdot 6H_2O$ (g/L)	60
H_3BO_3 (g/L)	30
Current density A (1 V)	0.02
Bath temperature (ºC)	60-80
pH	4.5-5.0

The distance between anode and cathode was kept constant at 20 mm. A schematic view of the electro deposition tank is shown in Fig. 1.
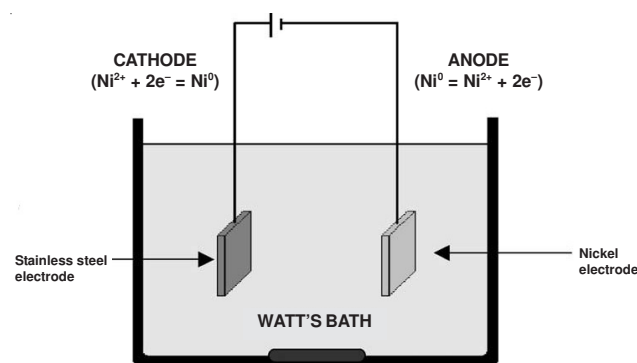

Fig. 1. Schematic view of the experimental set up used carry out electrochemical deposition of nickel on 304 stainless steel

The thickness of Ni plating was measured by optic micrometer. Nickel anode used for the plating was taken as 2 cm^2 surface areas (99.9 % purity) and all nickel plating was obtained under atmospheric condition[20-24].

Surface characterization: The surface morphology of the specimens were characterized using scanning electron microscopy (SEM) and energy dispersive X-ray analyzer (EDX) by using LEO 1430 VP model. The adsorption of the organic molecule to the substrate was examined using surface reflectance Fourier transform infrared spectroscopy (FT-IR-Perkin-Elmer BX-II model).

RESULTS AND DISCUSSION

Cyclic voltametry results: The values of y depend on the oxidation state of the polymer. Polyaniline (polyaniline, R = H) and its ring-substituted derivatives are known to have three oxidation states: fully reduced, leucoemeraldine (LE, y = 1); intermediately oxidized, emeraldine (E, y = 0.5) and fully oxidized, perni-graniline (PN, y = 0). Fig. 2 is given each of these states has a protonation degree depending on the solution pH and in the case of ring substitution on the steric hindrance and the electronic effect due to substituents[3,25-27].
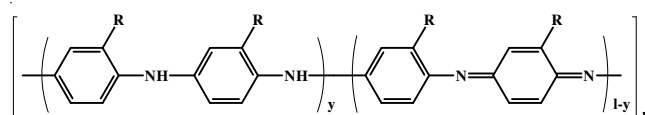

Fig. 2. Structure of polyaniline

Polyaniline coat was electrochemically synthesized using cyclic voltammetry on steel surface. The cyclic voltamograms, which were obtained for platinum and 304 steel electrodes in different scanning rate in 0.3 M oxalic acid and 0.3 M oxalic acid + 0.1 M aniline solutions, are shown in Fig. 3.
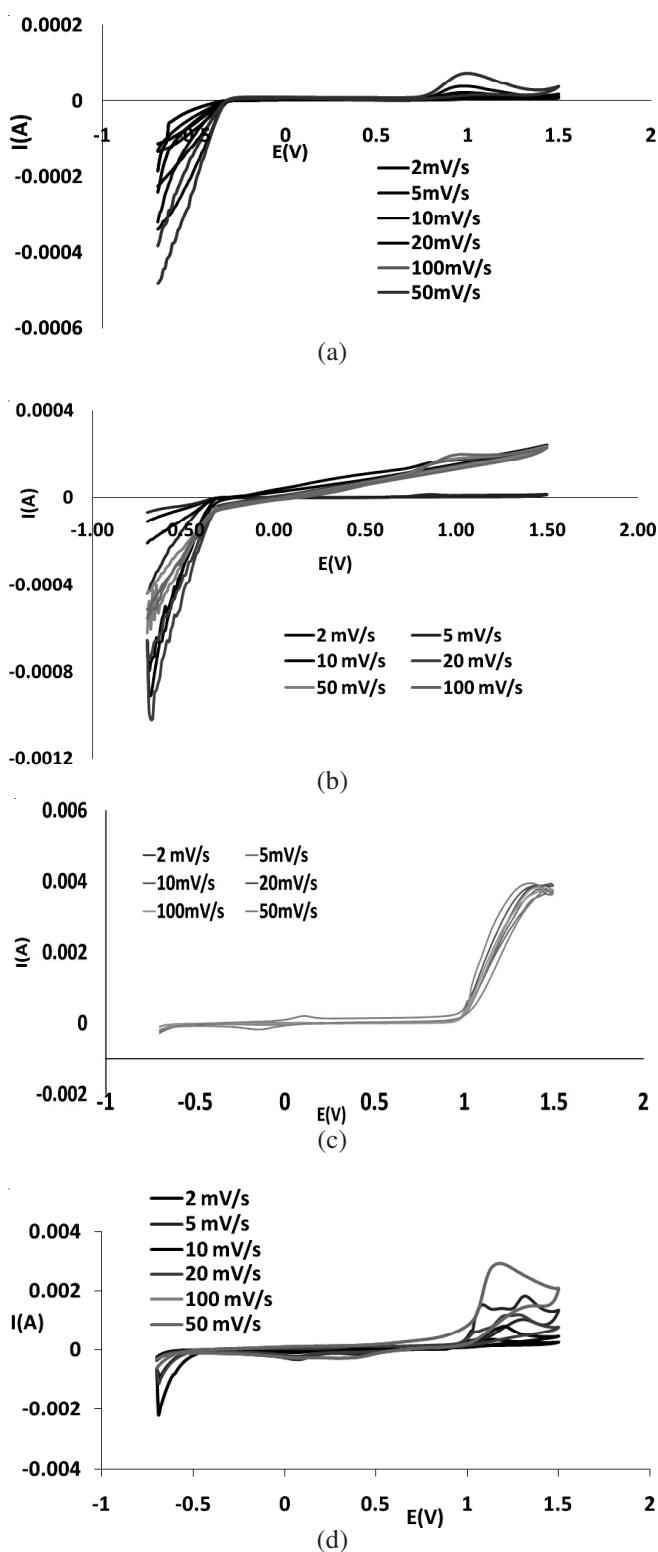

(a)

(b)

(c)

(d)

Fig. 3. Cyclic voltamograms obtained at different scan rates, (a) obtained in 0.3 M oxalic acid solution for Pt (b) obtained in 0.3 M oxalic acid + 0.1 M aniline solution for Pt (c) obtained in 0.3 M oxalic acid solution for 304 steel (d) obtained in 0.3 M oxalic acid +0.1 M aniline solution for 304 steel

The current increase after 0.8 V potential in 0.3 M oxalic acidic medium has indicated the PtO evolution (Fig. 3a). The passiveness range is approximately in the range 1.1 V in all scanning rates (Fig. 3a). As the scanning rate increases, the charge value passing through the surface has decreased from 1275 to 279 μC. This case shows that the metal surface is getting passive by coating through oxides (PtO). Approximately after 0.9 V, the increase of current values has been observed. This situation can be in the shape of degradation of passive oxide film or the break of it occurred in the surface. The increase of current except for passiveness current in the current potential curve can be explained as the transition to transpassive area. The metal is corroded through oxidation again in tranpassive area. It can be seen that the current is close to zero until 0.02 V potential (Fig. 3b) and it can be said that the peak, which is occurred because of the increase of current after 0.02 V potential, results from the oxidation of aniline. It can be observed that there is no passiveness range and there is a continuous current increase. The only peak observed in 0.8 V in 5 mV s^{-1} scanning rate can be because of PtO evolution (Fig. 3b).

The passiveness range on the steel is about 1.0 V (Fig. 3c). It is an enough potential range to form oxide film. An oxidation peak in about 0.150 V and a reduction peak in about -0.208 V can be observed only in 100 mV s^{-1} scanning rate. When the cyclic voltammogram taken from the -0.7 V and 1.5 V potential ranges is examined, it can be observed that about -0.15 V current values has increased. This shows that Fe^{2+} ions occurred in the decomposed area of the electrode incorporate with oxalate ions and it forms Fe(II) oxalate layer whose resolution is low ($K_{çç}$: 2.1×10^{-7}). As a result of this it can be said that the surface of electrodes are getting passive. The reactions of oxidation and oxalate precipitation processing on the electrode surface are as follow:

$$Fe \longrightarrow Fe^{2+} + 2e \qquad (1)$$

$$Fe^{2+} + C_2O_4^{2-} \longrightarrow FeC_2O_{4(solid)} \qquad (2)$$

If the reaction is organized by assuming that these reactions correspond to oxidation/passivation peak on the single peak, the following total reaction occurs:

$$Fe + C_2O_4^{2-} \longrightarrow FeC_2O_{4(solid)} + 2e^- \qquad (3)$$
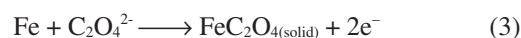
It is observed that the current density has increased after 1 V potential and there is also a peak in *ca.* 1.35 V. This case shows that there is oxygen gas evolution and the following reaction must occur, if its acidic medium is taken into consideration:

$$2H_2O \longrightarrow O_{2(g)} + 4H + 4e^- \qquad (4)$$
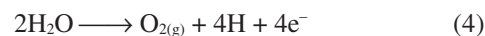
when Fig. 3d is examined, it is seen that there is a narrower potential range compared to oxalic acid medium although there is a passiveness range for 304 steel in 0.3 M oxalic acid + 0.1 M aniline solution. The passiveness range, which is included 20 mV s^{-1} scanning rate, is as wide as 1.0 V.

As the scanning rate increases, the decrease of charge amount through the system has supported oxide formation on polyaniline and steel surface. The oxidation peak, which is about 1.2 V, shows that polyaniline is oxidized to pernigraniline. As scanning rate increases, the value of oxidation peak current

has increased. This accelerates pernigraniline oxidation of polyaniline. The reduction peak, which is observed as *ca.* 0.5 V, results from the reduction of pernigraniline leucomeraldin form[28]. Voltamograms obtained for platinum and 304 steel after 50 cyclic in 0.3 M oxalic acid, 0.3 M oxalic acid + 0.1 M aniline solution and Ni coated 304 steel in 0.3 M oxalic acid +0.1 M aniline solution in 50 mV s^{-1} scanning rate are given in Fig. 4.
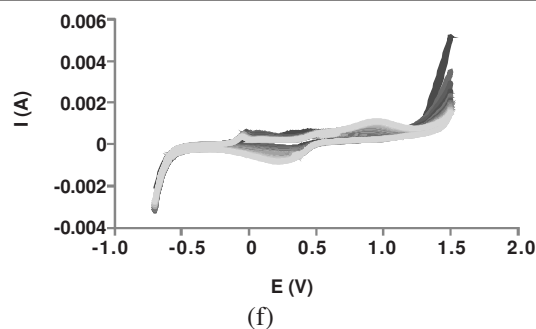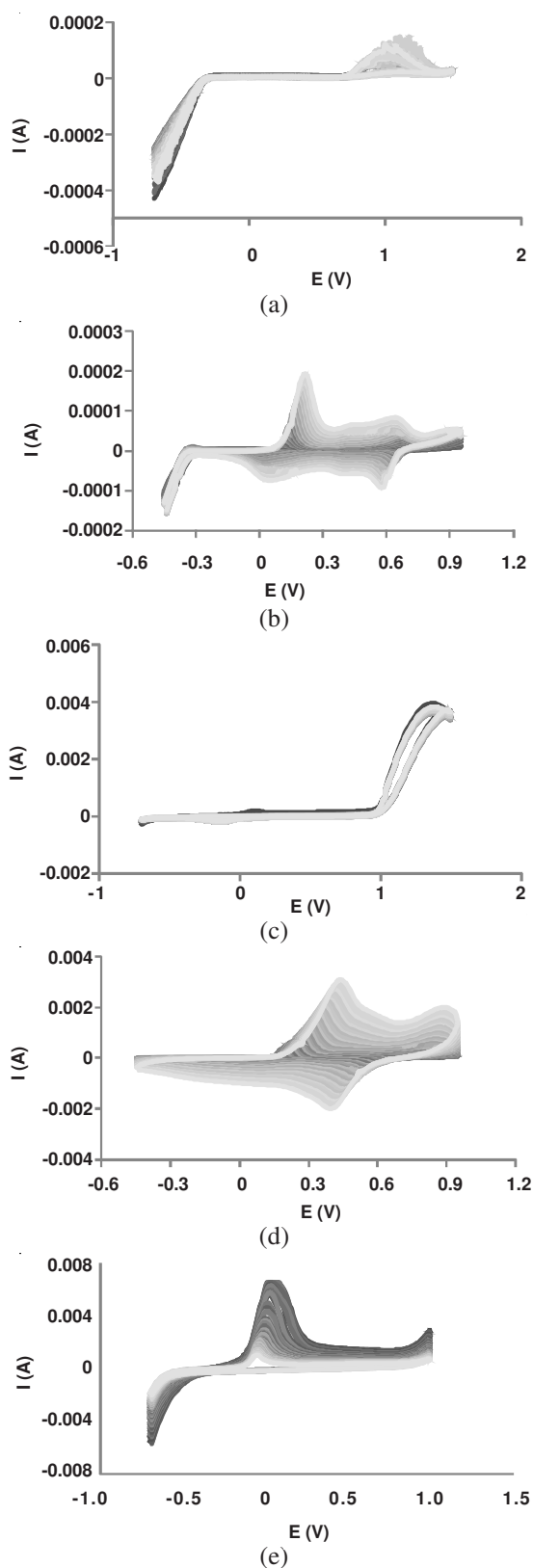

(a)

(b)

(c)

(d)

(e)

(f)

Fig. 4.   Voltamograms obtained in 50 mV s^{-1} scanning rate (50 cycles), (a) obtained in 0.3 M oxalic acid solution for Pt (b) obtained in 0.3 M oxalic acid +0.1 M aniline solution for Pt (c) obtained in 0.3 M oxalic acid solution for 304 steel (d) obtained in 0.3 M oxalic acid +0.1 M aniline solution for 304 steel (e) obtained in 0.3 M oxalic acid +0.1 M aniline solution for Ni plated 304 steel

When Fig. 4a is examined, the passiveness range is about 1 V. The current value of charge peak is 74 μA in about 0.1 V s^{-1}. As the cyclic number increases, the charge amount passing through the system is almost same until 30th cycle and it is about 504 μC. The charge amount has increased to 833 μC after the 30th cycle. The existence of passiveness range enables the aniline polymerization.

It is observed that the surface is passive until the 10th cycle in 0.3 M oxalic acid + 0.1 M aniline solution compared to Fig. 4b for Pt. After the 10th cycle, the first oxidation and the first reduction peak has started. As the cycle numbers increases, oxidation peak potentials have shifted to more positive potentials and current values have increased. As cycle numbers have increased, the reduction peak potentials have shifted to more negative values and the reduction current has increased[29]. The passiveness range has been observed from the 1st cycle to the 10th cycle. The first oxidation peak value has started from 0.1 V and it has shifted until 0.23 V in the 5th cycle. The current value has also increased continuously. The first reduction peak potential has increased about 0.7 V in the current. The first maximum peak has been observed as almost 0.1 V together with cycle number. It has declined sharply after that. After the 10th cycle, oxidation values have increased in the direction of positive. This case shows that that the process of monomer formation has shifted to lower potentials. The reduction of polyaniline film has been observed with the process of exchange of charge of cathodic area in reverse scanning.

At the reverse scan of first cycles, the reduction of polyaniline film was observed as current change in cathodic field. At the forward scan of the 2nd and 3rd cycles, the current changes related to polyaniline film reduction increased regularly with increasing cycle numbers due to film growth. The current values of repassivation peak are recorded for MS electrode relatively lower with respect to monomer free conditions (Fig. 4c). This event must have been caused by inhibitor effect of aniline on electrode surface. The intensity of repassivation peak decreased regularly with increasing cycle numbers (Fig. 4b). This could be explained with the thin polyaniline film which was produced on MS surface and the repassivation peak indicated to have the porous structure of polymer film. The broad peaks have been observed as about

0.25 V on Pt. The other peaks are determined as oxidation and reduction peaks of polyaniline because of the transition among oxidation stages. Those peaks, which are in response to oxidation and reduction, have increased in ratio to cycle number. The fact that the top potential limit is little higher than polyaniline degradation potential value (about 0.75 V) shows that degradation process is not as important as film growth.

When 50 cyclic voltamogram of 304 steel is examined in oxalic acid medium in 50 mV s⁻¹ scanning rate (Fig. 4c), it is observed that the passiveness range is between about 0.7 and +0.9 V. In only first cycle, it is also seen that it gives a oxidation peak in about 0.11 V and a reduction peak in about -0,15 V. In about 1.6 V potential range, the currents are very little on steel surface and this area can be taken as passiveness area[10]. Fig. 4d showed approximate one oxidation peak and two reduction peaks. This indicates the effect of the polyaniline. NiO current peak in approximate 0 Volts is observed in Fig. 4e, this current peak is removed after it is covered with metal polymer in an aniline media. This indicates the effect of polyaniline concealer.

The oxidation peaks are seen especially in the 20th cycle across SCE in 0.2 and 0.5 V show that polyaniline turns from leucoemeraildine into emeraldine and it transforms from emeraldine into pernigraniline. The one reduction peak in 0.4 V and 0 V reveal that polyaniline turns from pernigraniline into emeraldine and from emeraldine into leucoemeraldine[30-32]. When 50 cycles are totally investigated, it is observed that there is only one oxidation and only one reduction peak. It is also observed that the pernigraniline oxidation of polyaniline turns into pernigraniline leucoemeraldine in reverse cycle. polyaniline is oxidized because of metal polymer growth in the pores under the coating and it is reduced on metal polymer interface. These two cases provide the increase of coating resistance[33].

On examining of Fig. 4f, the formation of Fe(II) oxalate compound whose passiveness mechanism is decomposed on the steel is based on the formation of insoluble nickel oxalate on steel/Ni. The change of current has started in about 0.5 V in the following scanning. This case shows that Fe(II) oxalate compounds are composed of the decomposition of Fe(II) compounds. There is change between 0.4 V and 1.05 V on steel/Ni. The sharp peak in reverse peak at *ca.* 0.1 V is the peak of repasivization of steel electrode. This peak indicates the reduction of Fe(III) compounds to Fe(II) compounds. The oxidation of monomer on steel is approximately observed in 1.4 V in the 1st cycle. The passiveness mechanism of nickel is the insoluble nickel oxalate and nickel oxides[33]. And it is stated that Ni is chemically bonded (predicated) on polymer chain[7,34].

Tafel extrapolation and linear polarization results: In this study, Tafel curves of uncoated steel and polyaniline and Ni + polyaniline coated 304 steel in 3.5 % NaCl, 1 N NaOH and 1 N HCl solutions are also given in Fig. 5.

Fig. 5 is investigated it is seen that as waiting time increases, the value of i_{cor} has increased. This increase may result from the decomposition of passive iron oxalates occurred on the surface or it can be said that polyaniline coatings show a temporary resistance. When i_{cor} values of polyaniline coated steel is compared to that of uncoated steel, it is observed that i_{cor} values have increased on polyaniline coated steel (except 120 h). The increase of i_{cor} values is because of the
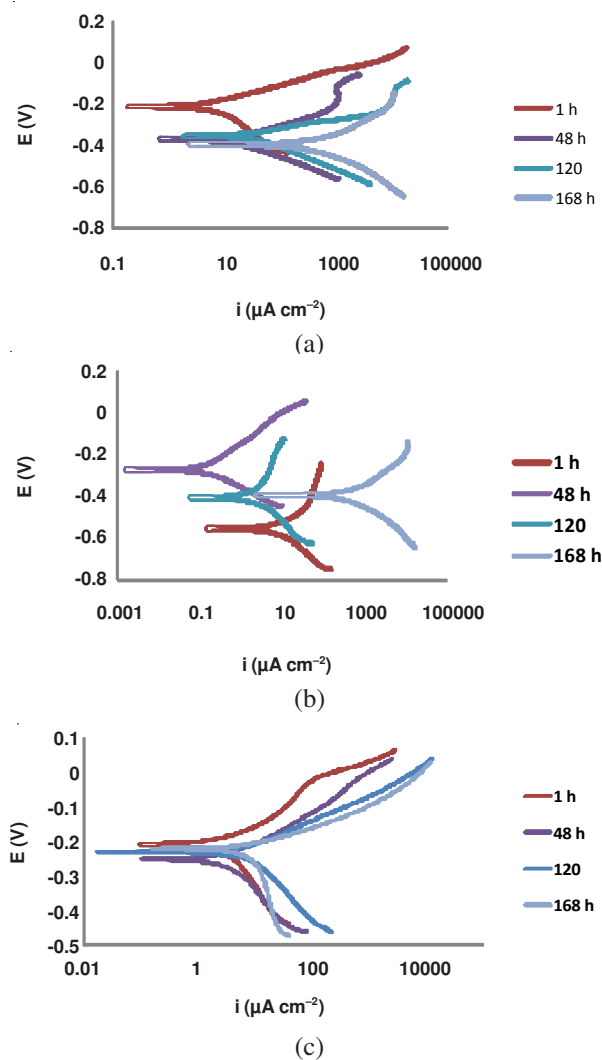

Fig. 5.   Tafel plots for Ni + polyaniline coated 304 steel in different solutions (a) 1 N HCl (b) 1 N NaOH (c) % 3.5 NaCl

conductivity of polyaniline film. This indicates that polyaniline does not adhesive to the surface exactly and it has a porous structure and it departs from its steel surface in the course of time by incorporating water to it structure and holding water process[6].

The corrosion characteristics of uncoated steel, polyaniline coated and Ni + polyaniline coated steel in 1 N HCl solution are given in Table-3. On examining Table-3, βa and βc values have taken higher values that uncoated surface in Ni + polyaniline coated steel. This case shows that the protection has increased.

i_{cor} values (except 120 h) have decreased on uncoated steel in 1 H HCl medium. The i_{cor} values have decreased until 48 h in polyaniline coating, they have started to increase from 120 and 168 h and in the course of time the current values have increased in Ni + polyaniline coating. In polyaniline coating, 48 h is observed as optimum period for the protection of surface. The increasing current values after 48 h show that the degradation of passive film composed of oxides on the surface. The porous structure of polyaniline has also an effect on this process. It is observed that the current values of Ni + polyaniline coating, except for 168 h, are lower than i_{cor} values on uncoated and polyaniline coated surfaces. Therefore, this case indicates

TABLE-3
ELECTROCHEMICAL CHARACTERISTICS OF 304 STEEL IN 1N HCl SOLUTION

	Waiting time (h)	βa (V/decade × 10^{-3})	βc (V/decade × 10^{-3})	i_{cor} (µA)	E_{cor} (mV)	Corrosion rate (mpy)	Rp (kΩ)	Eocp (mV)
Uncoated	1	65	90	15.0	-423	23.8	633×10^{-3}	-410.4
	48	43	74	6.8	-394	8.5	1.126	-384.6
	120	50	83	12.0	-360	28.0	205	-363.9
	168	35	68	3.20	-389	5.0	1.099	-388.0
PANI coated	1	63	122	9.5	-408	15.2	401×10^{-3}	-414.9
	48	51	73	5.8	-393	9.3	833×10^{-3}	-377.5
	120	56	86	8.2	-398	13.0	632×10^{-3}	-367.2
	168	56	71	11.5	-370	18.4	698×10^{-3}	-353.7
Ni + PANI coated	1	107	158	2.0	-214	3.2	10.86	-182.1
	48	77	99	4.1	-371	6.5	3.02	-309.9
	120	61	96	8.6	-356	13.7	975×10^{-3}	-337.6
	168	92	107	84.0	-400	134.0	189×10^{-3}	-398.7

TABLE-4
ELECTROCHEMICAL CHARACTERISTICS OF 304 STEEL IN 1N NaOH SOLUTION

	Waiting time (h)	βa (V/decade × 10^{-3})	βc (V/decade × 10^{-3})	i_{cor} (µA)	E_{cor} (mV)	Corrosion rate (mpy)	Rp (kΩ)	Eocp (mV)
Uncoated	1	230	143	72×10^{-3}	-288	114×10^{-3}	150	-223.6
	48	98	69	5.8×10^{-3}	-342	72.3×10^{-3}	8.5	-234.7
	120	151	108	25×10^{-3}	-367	61×10^{-3}	165	-308.5
	168	122	115	57×10^{-3}	-329	92×10^{-3}	42	-292.7
PANI coated	1	120	122	9.5	-408	15.20	575	-414.9
	48	51	73	5.8	-393	9.3	1.2×10^{3}	-377.5
	120	56	86	8.2	-398	13	220	-367.2
	168	56	71	11.5	-370	18.4	1.2×10^{3}	-353.7
Ni + PANI coated	1	155	165	2.6	-555	4.1	12.01	-497.2
	48	232	110	59×10^{-3}	-278	94×10^{-3}	451	-201.4
	120	180	293	2.05	-410	3.26	49.39	-377.3
	168	158	444	4.07	-334	6.5	48.47	-287.5

that Ni + polyaniline coating shows better corrosion resistance. The corrosion characteristics of uncoated 304 steel, polyaniline and Ni + polyaniline coated 304 steel in 1 N NaOH solution are given in Table-4.

When E_{cor} values of Ni + polyaniline are compared with uncoated surface (Table-4), it is seen that they have shifted to more negative values. This case shows that Ni + polyaniline has decreased the corrosion because of cathodic depolarizator effect. The corrosion characteristics of uncoated 304 steel, polyaniline and Ni + polyaniline coated 304 steel in 3.5 % NaCl solution solution are given in Table-5.

The i_{cor} values in Ni + polyaniline coating have increased compared to uncoated surface. It can be said that Cl⁻ ions existed in 3.5 % NaCl solution cause pitting corrosion in its steel surface by diffusing from the coatings. The E_{cor} values of Ni + polyaniline coating have shifted to more negative potential values compared to its steel surface except 48 h. When polyaniline and Ni + polyaniline are compared, i_{cor} values have decreased in Ni + polyaniline except 48 and 120 h. This case can be explained that Ni + polyaniline coating shows better corrosion resistance that polyaniline on steel. The reason of having no protection in 168 h is to have a protection of polyaniline coating for 2-5 days and to have no protection of it after 5 days. Also the formation of galvanic corrosion between nickel coating and steel increases this situation.

Potansiostatic impedance results: The Nyquist plots for 304 steel in 3.5 % NaCl solution are given Fig. 6.
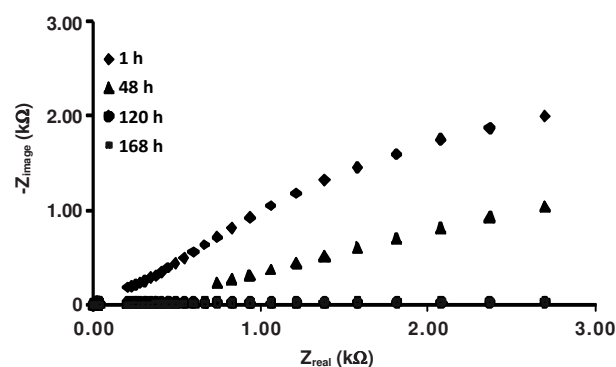
(a)

(b)

TABLE-5
ELECTROCHEMICAL CHARACTERISTICS OF 304 STEEL IN 3.5 % NaCl SOLUTION
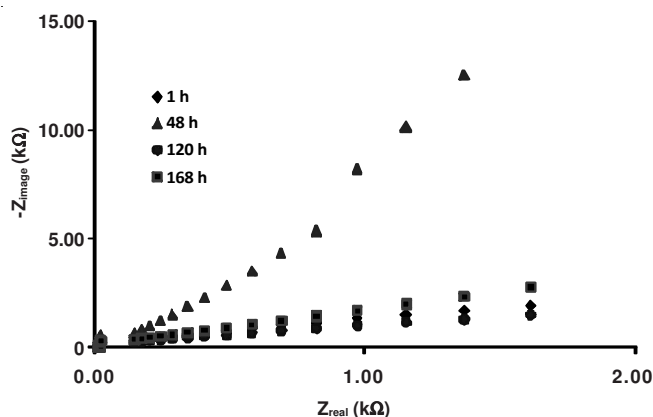
	Waiting time (h)	βa (V/decade × 10^{-3})	βc (V/decade × 10^{-3})	i_{cor} (µA)	E_{cor} (mV)	Corrosion rate (mpy)	Rp (kΩ)	Eocp (mV)
Uncoated	1	101.0	70.1	73.2×10^{-3}	- 152	116×10^{-3}	141.50	-58.6
	48	72.2	49.4	15×10^{-3}	- 289	19×10^{-3}	8.20	-210.8
	120	210.0	112.0	14×10^{-3}	- 149	33.9×10^{-3}	451.00	-91.2
	168	114.0	85.0	55×10^{-3}	- 206	87.5×10^{-3}	65.00	-153.4
PANI coated	1	198.0	155.0	3.145	- 162	5	176.00	-84.8
	48	322.0	230.0	1.180	- 207	1.718	27.99	-155.5
	120	233.0	166.0	15×10^{-3}	- 140	36.3×10^{-3}	334.00	-91.2
	168	170.0	241.0	7.75	- 243	12.3	34.50	-199.2
Ni + PANI coated	1	88.0	198.0	880×10^{-3}	- 211	1.4	22.92	-187.7
	48	98.0	206.0	1.26	- 253	2	17.81	-213.2
	120	93.0	183.0	2.70	- 234	4.3	7.69	-212.7
	168	52.0	265.0	2.13	- 222	3.4	3.65	-222.2
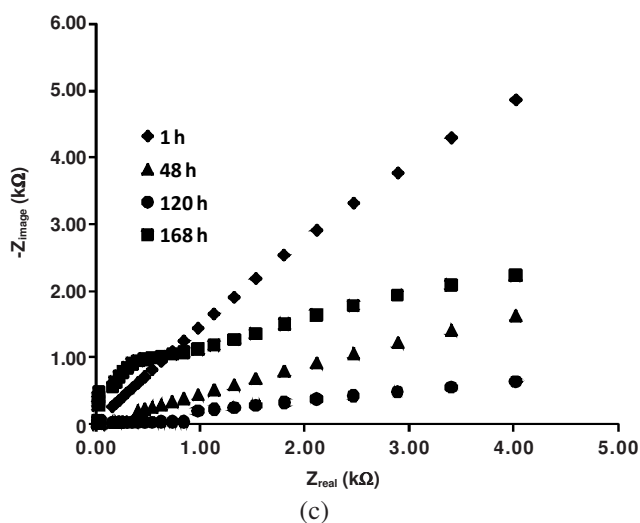
Fig. 6.   The Nyquist and Bode plots for Ni + polyaniline coated 304 steel in different solutions (a) 1N HCl (b) 1N NaOH (c) % 3.5 NaCl

When Fig. 6 is investigated, it is seen that the impedance of polyaniline coated steel has decreased in the course of time. This case demonstrates that polyaniline coating occurred on the surface does not protect the surface exactly and it has a porous structure and the corrosion has increased on the surface through enabling especially chlorine passing by corrosive ions.

Charge transfer resistance is responsible for anodic dissolution occurred with the pores of uncoated sample surface and nickel coating. The diameter of semi cycle for uncoated metal is polarization resistance (Rp) is charge transfer resistance (R_{ct}).

The decrease of capacity values on polyaniline coated one indicates that the protection of the coating continues. The decrease of charge transfer resistance of Ni + polyaniline coating is because of having low decomposition of iron. However, the increase of passive film has resulted in firming of R_{ct} value. The fact that the decrease of impedance value in the course of time and having no change of charge transfer resistance values in 1 and 48 h and the decrease of it later on demonstrates that polyaniline surface protects the surface simply for 48 h. This case is confirmed with the literature[35].

Anodic oxidation of nickel under the catalyzes of polymer film can be also explained as the transforming from charge transfer resistance to its oxides in high frequencies. The linear part, which is occurred in low frequencies in EIS Nyquist

curves, can be determined as the diffusion of corrosion products passing through the pores of polyaniline film and oxide layer. Anodic oxidation of nickel under the catalyzes of polymer film can be also explained as the transforming from charge transfer resistance to its oxides in high frequencies. The catalytic effect of polymer coating and coated metal should be taken into consideration in solution interface. Electrochemical processes have occurred as following:

$$Ni \longrightarrow Ni^{2+} + 2e \qquad (6)$$
$$EM^{2+} + 2e \longrightarrow LEM \qquad (7)$$
$$2O_2 + H_2O + 2e \longrightarrow 2OH^- \qquad (8)$$
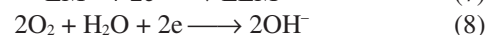
In equation 7, EM is emeraldin, LEM is leucoemeraldine. The reduction of polymer film has assisted in the increase of solution resistance value. Polymer film and nickel, which is occurred before and together with oxide layer show an effect of barrier on steel corrosion. In the longer period, this barrier effect has decreased by diffusion of Cl⁻. Polyaniline coating has increased the barrier effect by closing the pores of nickel.

Surface analysis results: EDX spectrums of uncoated, Ni coated, polyaniline coated and Ni + polyaniline coated 304 steel are given in Fig. 7 (Table-6).

TABLE-6
VALUES OF EDX FIELD SCANNING (% ATOM)

% ATOM	Uncoated	PANI coated	Ni coated	Ni + PANI coated
Carbon	–	17.75	–	26.73
Oxygen	–	55.11	76.80	51.59
Iron	73.96	4.97	–	–
Nickel	7.32	3.78	14.70	6.59
Sulphur	–	2.45	4.97	1.47
Chlorine	–	2.61	3.52	0.22
Chromium	18.72	1.21	–	–
Nitrogen	–	12.14	–	13.41

When Fig. 7 (Table-6) are examined, it is seen that carbon value has decreased according to polyaniline coated steel. The iron, oxygen, nickel and sulfur seen on polyaniline coated steel occurs on the surface because of steel structure. This case shows that polyaniline coating is not homogenous and has a porous structure. While there is no oxygen on the surface of uncoated steel, the oxygen amount on uncoated steel is very high. This case shows that polyaniline coating accelerates the oxidation of steel surface and supports the formation of passive

film on the surface. The nitrogen amount existed in polyaniline coating results from aniline chemical structure[36]. Oxygen, nickel sulfur and chlorur ions on nickel coating of surface have increased (Fig. 7b,d). This case is related on the compounds of Watt bath used in nickel coating studies. The increase of carbon and nitrogen on the surface of Ni + polyaniline coating has resulted from aniline (Fig. 7d). Ni + polyaniline dual coating (compared to single polyaniline and nickel coating) shows better surface characteristics. The surface becomes more homogenous and porous structures get closed. These findings are confirmed with the fact that Ni + polyaniline coating shows better corrosion resistance in Tafel tables and impedance plots.

(a)

(b)

(c)

(d)
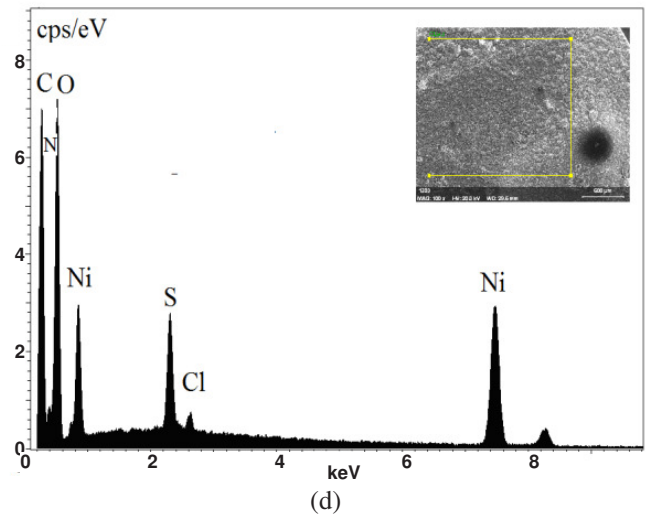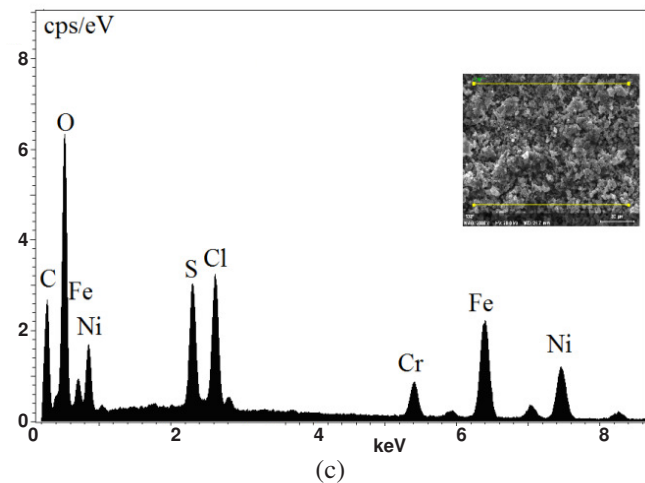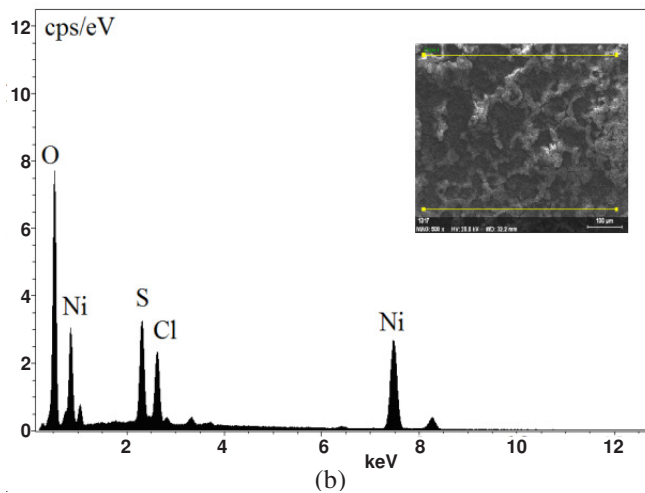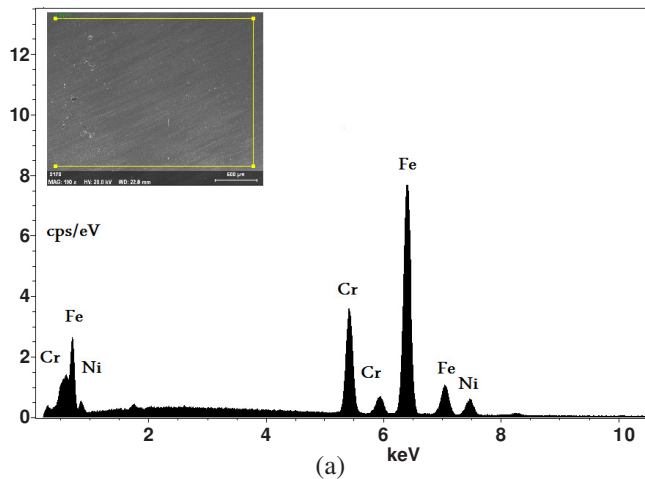
Fig. 7. EDX spectrums for 304 steel (a) uncoated (b) Ni coated (c) polyaniline coated d) Ni + polyaniline coated

SEM microphotographs of uncoated 304 steel, polyaniline coated steel, Ni + polyaniline coated steel surfaces are given in Fig. 8.

Fig. 8 shows that the uncoated metal surface (Fig. 8a,b) is homogenous and there are sandpapering defects. It is observed that the surface gets completely closed on polyaniline coated steel enlarged 2500 (Fig. 8c,d), however it has a porous structure. The images like geometrical structure in SEM images show iron oxalates occurred on 304 steel surface(Fig. 8e,f)[10]. SEM microphotographs of Ni coated steel, Ni + polyaniline coated steel surfaces are given in Fig. 9.
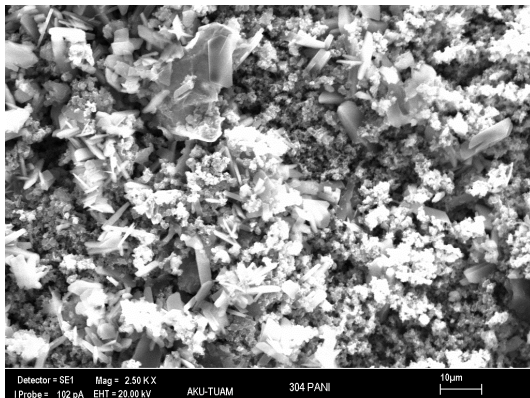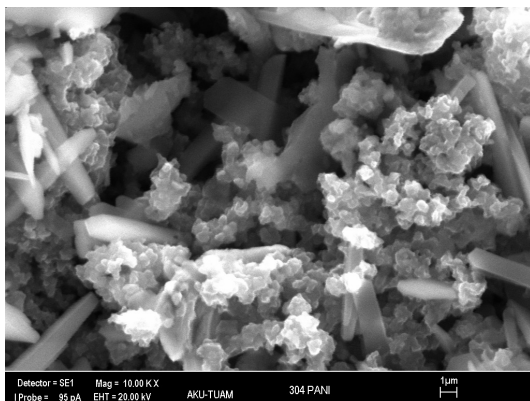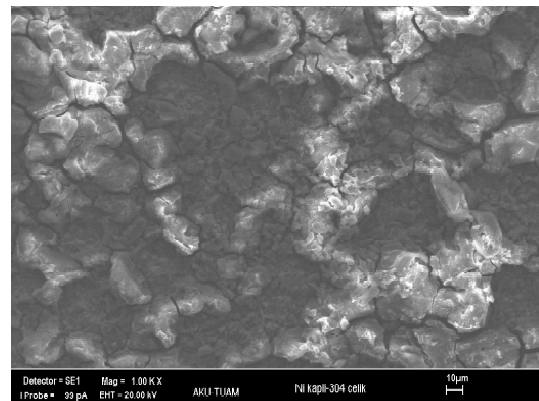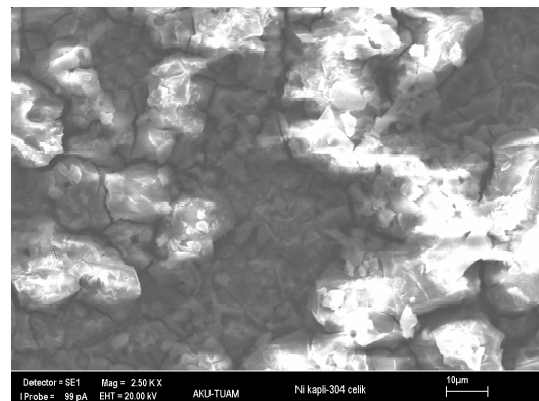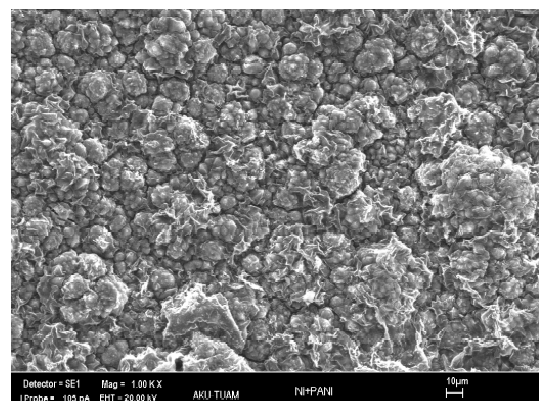

(a)

(b)

(c)

(a)

(d)

(b)

(e)

(c)

(f)

(d)
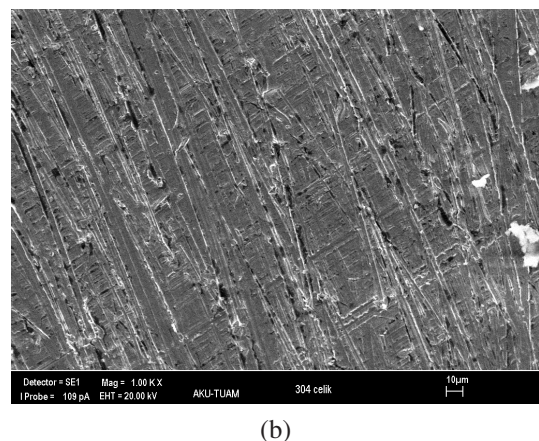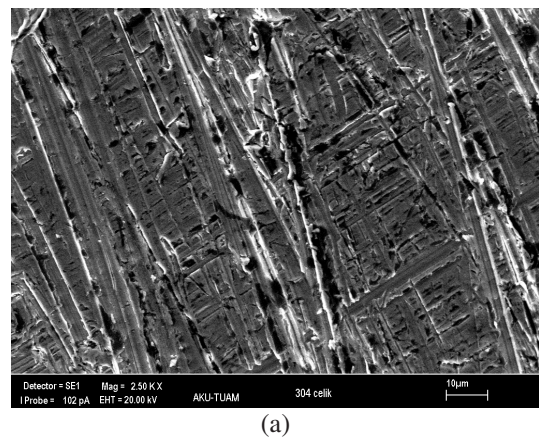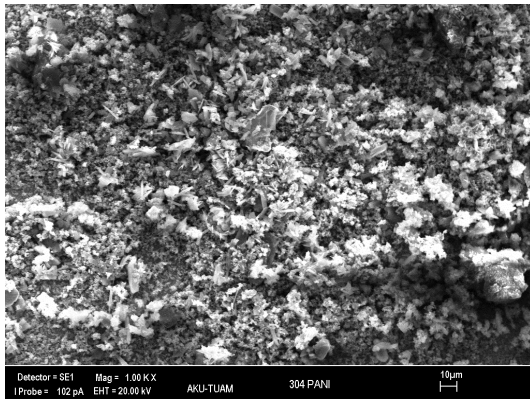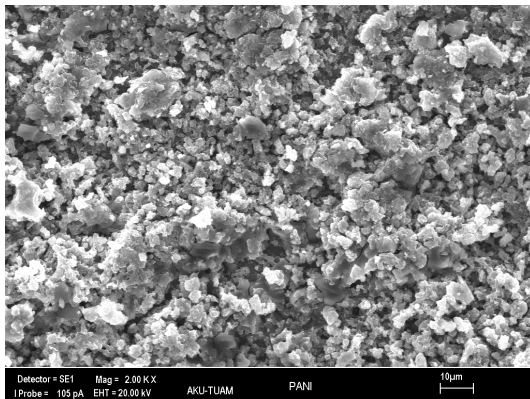
Fig. 8.   SEM microphotograps of uncoated and polyaniline coated 304 steel (a) uncoated 304 steel x 2.500, (b) uncoated 304 steel x 1.000, (c) polyaniline coated 304 steel x1.000, (d) polyaniline coated 304 steel x 2.500, (d) polyaniline coated 304 steel x 10.000
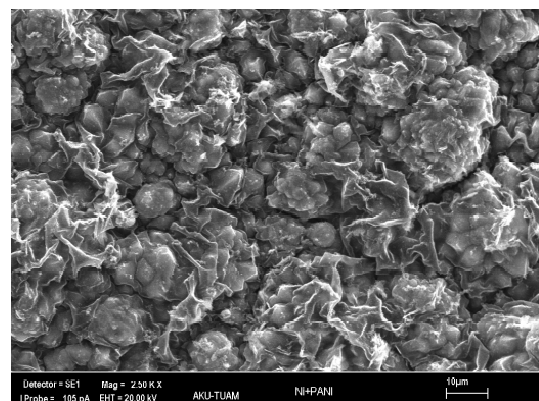
Fig. 9.   SEM microphotograps of 304 steel (a) Ni coated 304 steel x 1.000, (b) Ni coated 304 steel x 2.500, (c) Ni + polyaniline coated 304 steelx 1.000, (d) Ni + polyaniline coated 304 steel x 2.500

When Fig. 9 is examined, it is seen that the surface of nickel coating obtained by using electrochemical Watt bath gets completely closed by nickel (Fig. 9a,b). Not having a homogenous structure of nickel coating leads to better holding of polyaniline to the surface. The film thicknesses of nickel coating and Ni + polyaniline coating occurred on the surface (Fig. 9c,d) are measured by optic micrometer connected to OLYMPUS BX60 model metal microscope. The film thickness of Ni coating is measured as 14 μm. The film thickness of Ni + polyaniline coating is measured as 25 μm. The ranges which are observed in Ni + polyaniline coating in nickel coating are filled by polyaniline and more smooth and homogenous structure are obtained. As a result of this, corrosion resistances become higher (Tables 3-5).

FTIR Analyses results: FTIR spectrum of polianiline from taken off polyaniline coated 304 steel surface. Anilin monomer FTIR analysis is made by using distilled aniline. Spectrum of aniline monomer is given in Fig. 10. Spectrum of polyaniline is given in Fig. 11.
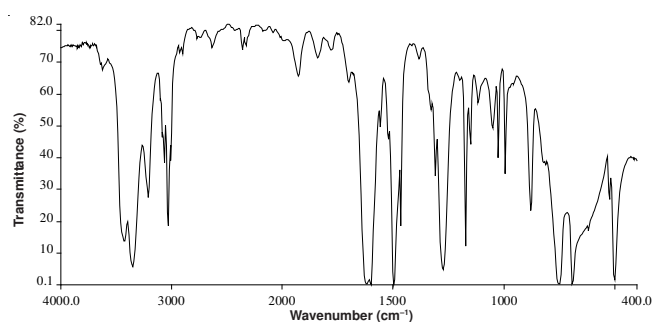

Fig. 10. FTIR spectrum of aniline monomer

Fig. 10 showed standard aniline monomer spectrum. When FTIR spectrum of polyaniline (Fig. 11) is examined, 3000-2800 cm^{-1} C-H stretching peak, 1730-1250 cm^{-1} C-O stretching peak, the peaks related to 1607, 1581, 1510 cm^{-1} aromatic structure shows 551-431 cm^{-1} ferrite structure. C-N stretching in 1308 cm$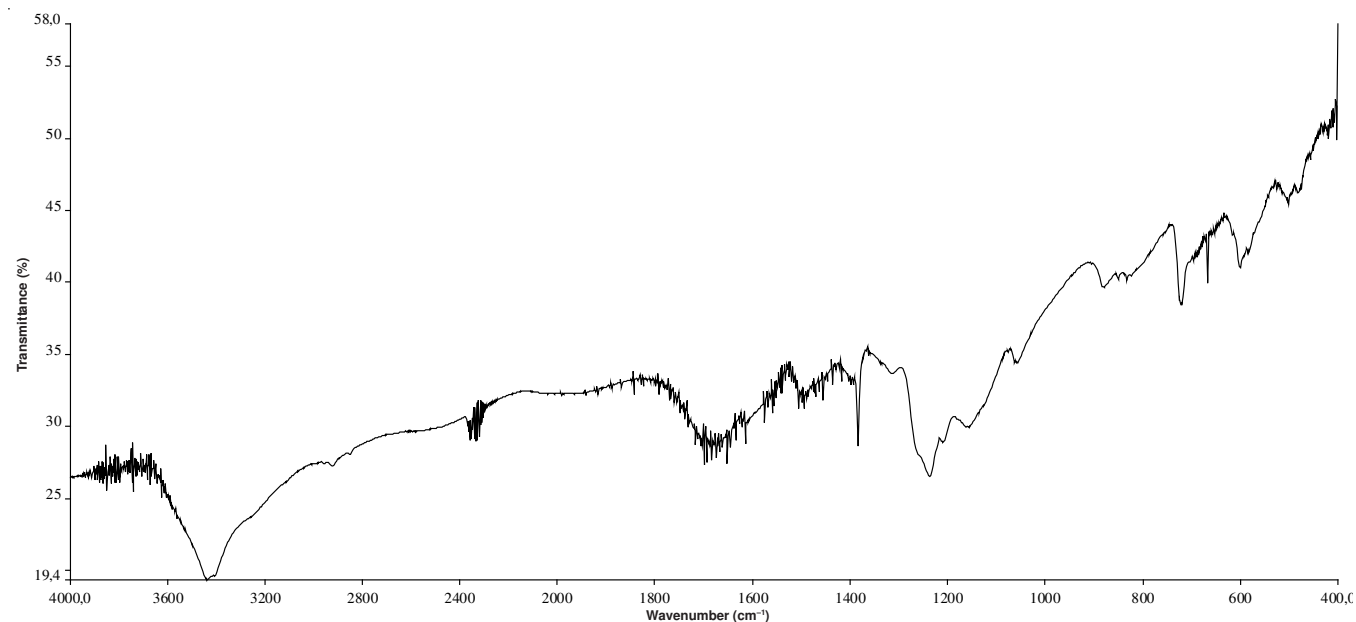^{-1}$ indicates secondary aromatic amine structure. 1559 cm^{-1} C=C ring stretching and other additional peaks are related to the coordination of polymer chain[3,7,35,37,38].

Conclusion

(1) The oxidation peak potentials in all cyclic voltamograms have shifted to more positive potentials as the cyclic numbers increase and current values have also increased. On the other hand, reduction peak potentials have shifted to more negative values and reduction current increases. This case shows that there have been polymer occurrence and the occurrence reaction of polyaniline is autocatalytic.

(2) It is observed that there is single oxidation and single reduction peak in 50 cyclic voltamograms in 0.3 M oxalic + 0.1 M aniline solution of 304 steel. And it seen that the pernigraniline oxidation of polyaniline is transformed into pernigraniline leucoemeraldine in reverse cyclic. polyaniline is oxidized in the pores under the coating because of growth of metal polymer and it is reduced in metal polymer interface. These two cases cause the increase of resistance.

(3) The fact that i$_{cor}$ values in polyaniline coated steel is higher than that of uncoated and Ni + polyaniline coated steel shows that polyaniline has not held to the surface completely and it has a porous structure. In the course of time it can be said that it become fatter by absorbing water into its structure and it departs its steel surface.

(4) Galvanic corrosion between nickel and iron is one of the biggest problems encountered in the process of nickel coating. The pores occurred during the process of coating supports this case.

(5) polyaniline coating facilitates the oxidation of steel surface and supports the formation of passive film on the surface. Nickel + polyaniline coating, the increase of carbon and nitrogen results from aniline on the surface.

(6) SEM images show that is observed that the surface is filled in polyaniline coated steel, but it has porous structure. The images alike geometric structures in SEM images reveal that iron oxalates occurred on 304 steel surface. The pores observed in nickel + polyaniline coating and in nickel coating

Fig. 11. FTIR spectrum of polianiline from taken off PANI coated 304 steel surface

are filled with polyaniline and flatter and more homogenous structure is obtained. As a result of this corrosion resistance has become higher.

(7) When FTIR spectrum is examined the peaks related to 1607, 1581, 1510 cm^{-1} aromatic structure show 551-431 cm^{-1} ferrite structure. C-N stretching in 1308 indicates secondary aromatic amine structure. 1559 cm^{-1} C=C ringed stretching and other additional peaks are related to the coordination of polymer chain.

ACKNOWLEDGEMENTS

REFERENCES

1. N.L.D. Somasiri and A.G. MacDiarmid, *J. Appl. Electrochem.*, **18**, 92 (1988).
2. T. Osaka, S. Ogano, K. Naoi and N. Oyama, *J. Electrochem. Soc.*, **136**, 306 (1989).
3. S. Joseph, J.C. McClurea, R. Chianellia, P. Picha and P.J. Sebastian, *Int. J. Hydrogen Ener.*, **30**, 1339 (2005).
4. M.T. Nguyen and L.H. Dao, *J. Electrochem. Soc.*, **136**, 2131 (1989).
5. A. Kitani, J. Yano and K. Sasaki, *J. Electroanal. Chem.*, **209**, 227 (1986).
6. W.S. Araujo, I.C.P. Margarit, M. Ferreira, O.R. Mattos and P.L. Neto, *Electrochim. Acta*, **46**, 1307 (2001).
7. K.R. Prasad and N. Munichandraiah, *Synth. Met.*, **143**, 459 (2001).
8. D. Sazou and C. Georgolios, *Synth. Met.*, **81**, 429 (1997).
9. J.L. Camalet, J.C. Lacroix, S. Aeiyach, K.I. Chane-Ching and P.C. Lacaze, *Synth. Met.*, **102**, 1386 (1999).
10. N.M. Martyak, P. McAndrew, J.E. McCaskie and J. Dijon, *Prog. Org. Coat.*, **45**, 23 (2002).
11. K.G. Thompson, C.J. Bryan, B.C. Benicewicz and D.A. Wrobleski, *Polym. Prepr.*, **35**, 265 (1994).
12. N. Ahmad and A.G. MacDiarmid, *Synth. Met.*, **78**, 103 (1996).
13. N.V. Krstajic, B.N. Grgur, S.M. Jovanovic and M.V. Vojnovic, *Electrochim. Acta*, **42**, 1685 (1997).
14. A.A. Pud, G.S. Shapoval, P. Kamarchik, N.A. Ogurtsov, V.F. Gromovaya, I.E. Myronyuk and Yu.V. Kontsur, *Synth. Met.*, **107**, 111 (1999).
15. Y. Wei, J. Wang, X. Jia, J.M. Yeh and P. Spellani, *Polymer*, **36**, 4535 (1995).
16. J.R. Santos Jr., L.H.C. Mattoso and A.J. Motheo, *Electrochim. Acta*, **43**, 309 (1998).
17. A.G. MacDiarmid and N. Ahmad, US Patent 5 645 890 (1997).
18. P.C. Lacaze, C.A. Ferreira and S. Aeiyach, French Patent 9214092 (1992) to PSA Citröen and ITODYS.
19. P.C. Lacaze, J. Petitjean, S. Aeiyach and Mir-Hedayatullah, French Patent 9315385 (1993) to Sollac and ITODYS.
20. J.M. Molina, R.A. Saravanan, J. Narciso and E. Louis, *Mater. Sci. Eng.*, **383**, 299 (2004).
21. B. Szczygiel and M. Kolodziej, *Electrochim. Acta*, **50**, 4188 (2005).
22. R.Q. Fratari and A. Robin, *Surface Coat. Technol.*, **200**, 4082 (2006).
23. R. Mishra, B. Basu and R. Balasubramaniam, *Mater. Sci. Eng.*, **373**, 370 (2004).
24. M. Gavrila, J.P. Millet, H. Mazille, D. Marchandise and J.M. Cuntz, *Surface Coat. Technol.*, **123**, 164 (2000).
25. D. Sazou, *Synth. Met.*, **118**, 133 (2001).
26. Y.J. Ren and C.L. Zeng, *J. Power Sources*, **182**, 524 (2008).
27. D. Kowalski, M. Ueda and T. Ohtsuka, *Corros. Sci.*, **49**, 1635 (2007).
28. H.H.S. Javadi, F. Zuo, K.R. Cromack, M. Angelopoulos, A.G. MacDiarmid and A.J. Epstein, *Synth. Met.*, **29**, 409 (1989).
29. S. Gottesfeld, A. Redondo, I. Rubinstein and S.W. Feldberg, *J. Electroanal. Chem.*, **265**, 15 (1989).
30. E.M. Genies and C. Tsitavis, *J. Eletroanal. Chem.*, **195**, 109 (1985).
31. A.J. MacDiarmid, P. Pouget, C.H. Hsu and A.G. Epstein, *Synth. Met.*, **69**, 119 (1995).
32. N. Pekmez, K. Pekmez and A. Yildiz, *J. Electroanal. Chem.*, **370**, 223 (1994).
33. A.T. Özyilmaz, G. Kardas, M. Erbil and B. Yazici, *Appl. Surf. Sci.*, **242**, 97 (2005).
34. T. Zalewska, A. Lisowska-Oleksiak, S. Biallozor and V. Jasulaitiene, *Electrochim. Acta*, **45**, 4031 (2000).
35. S. Sathiyanarayanan, S. Muthukrishnan, G. Venkatachari and D.C. Trivedi, *Prog. Org. Coat.*, **53**, 297 (2005).
36. K. Ding, Z. Jia, W. Mac, R. Tong and X. Wang, *Mater. Chem. Phys.*, **76**, 137 (2002).
37. S. Sathiyanarayanan, S. Muthukrishnan and G. Venkatachari, *Electrochim. Acta*, **51**, 6313 (2006).
38. S. Sathiyanarayanan, S.S. Azim and G. Venkatachari, *Electrochim. Acta*, **53**, 2087 (2008).